HHS Public Access

Author manuscript

Frequency-Driven Self-Organized Helical Superstructures Loaded with Mesogen-Grafted Silica Nanoparticles

Karla G. Gutierrez-Cuevas[‡,a], **Dr. Ling Wang**[‡,a], **Dr. Zhi-gang Zheng**[a], **Dr. Hari K. Bisoyi**[a], **Prof. Guoqiang Li**[b], **Dr. Loon-Seng Tan**[c], **Dr. Richard A. Vaia**[c], and **Prof. Quan Li**[a,*]

[a]Liquid Crystal Institute and Chemical Physics Interdisciplinary Program, Kent State University, Kent, Ohio 44242, United States

[b]Department of Ophthalmology and Visual Science and Department of Electrical and Computer Engineering, Ohio State University, Columbus, Ohio 43212, United States

[c]Materials and Manufacturing Directorate, Air Force Research Laboratory, Wright-Patterson AFB, Ohio 45433, United States

Abstract

Adding colloidal nanoparticles into liquid crystal media has become a promising pathway either to enhance or to introduce novel properties for improved device performance. Here we designed and synthesized new colloidal hybrid silica nanoparticles passivated with a mesogenic monolayer on the surface to facilitate their organo-solubility and compatibility in liquid crystal host. The resulting nanoparticles were identified by ^{1}H NMR, TEM, TGA and UV-Vis techniques, and the hybrid nanoparticles were doped into a dual frequency cholesteric liquid crystal host to appraise both their compatibility with the host and the effect of the doping concentration on their electro-optical properties. Interestingly, the silica nanoparticle doped liquid crystalline nanocomposites were found to be able to dynamically self-organize into a helical configuration and exhibit multi-stability, *i.e.*, homeotropic (transparent), focal conic (opaque) and planar states (partially transparent), depending on the frequency applied at sustained low voltage. Significantly, a higher contrast ratio between the transparent state and scattering state was accomplished in the nanoparticle-embedded liquid crystal systems.

Graphical abstract

[*]Correspondence to: qli1@kent.edu (Q. L.).
[‡]These authors contributed equally to this work.
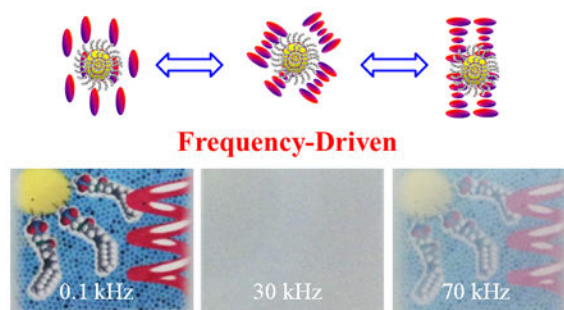
Frequency-Driven

Frequency-driven self-organized helical superstructures are fabricated by incorporating novel mesogen-grafted silica nanoparticles into a dual frequency cholesteric liquid crystal host. The resultant nanocomposites were able to exhibit multiple stable states, *i.e.*, transparent, opaque, and partially transparent, depending on the frequency applied at sustained low voltage. This work offers an impetus in developing dynamic functional soft materials potentially for diverse device applications such as smart windows.

Keywords

frequency-driven; hybrid silica nanoparticles; tunable transparency; self-organized helical superstructure; dual frequency liquid crystal

Cholesteric liquid crystals (LCs) with a self-organized helical disposition of molecules not only exhibit fascinating scientific phenomena but also have found practical applications in devices such as temperature sensors, reflective displays, color filters, mirrorless lasers and light shutters.[1] Recently, cholesteric LCs fabricated from nematic dual frequency LCs (DFLCs) with frequency dependence of the dielectric anisotropy have attracted considerable attention because both focal conic and planar configuration of such dual frequency cholesteric LCs (DFCLCs) can be switched depending on the frequency of the applied voltage, developing cholesteric reflective displays, fast switching bistable light shutters and bistable intensity modulators *etc.*[2] On the other hand, embedded metallic, semiconducting, and carbon nanomaterials have recently been employed to modify the properties of LCs.[3] It should be noted that dielectric silica (SiO_2) nanoparticles are the early examples of nanoparticle dispersions into LC matrices.[4] An advantage of SiO_2 nanoparticles in LCs is the modulation of the refractive index of LC media, which could be exploited to develop hybrid liquid crystalline nanocomposites with improved properties.[5] Though commercially available SiO_2 nanoparticles were able to modify some properties of LCs, their dispersions were not stable and only very small amount of the particles can be dispersed because of their strong propensity to aggregate or poor compatibility in LC matrix.[6] To circumvent this difficulty, surface functionalization of SiO_2 nanoparticles has been adopted which led to some interesting results.[7] Nevertheless, their functionalization with mesogenic or pro-mesogenic moieties is still a challenging task from the synthetic point of view, albeit this strategy could enable good dispersion and compatibility in LC media.[8] Here we functionalized SiO_2 nanoparticles with a covalently attached mesogenic monolayer through silane coupling agents and investigated their effect on the electro-optical property of a DFCLC system. The resulting hybrid nanoparticles (M-SiO_2) were organo-soluble without

noticeable aggregation and were able to disperse well in the DFCLC host with the concentration as high as 3.0 wt%. Interestingly, M-SiO$_2$ nanoparticles enabled to greatly enhance the electro-optical properties compared to the pure DFCLC. The light transmittance of the M-SiO$_2$ embedded LC nanocomposite films can be easily tuned by simply modulating the frequency of an applied constant voltage. Moreover, the M-SiO$_2$ doped system exhibited a higher contrast ratio compared with the pure DFCLC. To the best of our knowledge, this is for the first time that the effect of mesogen-grafted SiO$_2$ nanoparticles embedded in a dual frequency LC matrix is explored.

The synthesis of M-SiO$_2$ nanoparticles is straightforward in a facile manner as depicted in Scheme 1. The commercially available SiO$_2$-OH nanoparticles were reacted with (3-amino propyl)-triethoxy silane (APTES) in ethanol to afford the intermediate SiO$_2$-NH$_2$ nanoparticles followed by coupling with mesogenic 4-octyl-4-biphenylcarboxylic acid through the amide bond linkage. The resulting nanoparticles M-SiO$_2$ were characterized by proton nuclear magnetic resonance (^{1}H NMR), thermogravimetric analysis (TGA), transmission electron microscopy (TEM), energy dispersive X-ray spectrum (EDX) and UV-Vis analysis. The M-SiO$_2$ nanoparticles were able to well disperse in organic solvents such as THF and CHCl$_3$ even after being stored for several weeks at room temperature. ^{1}H NMR spectrum of M-SiO$_2$ nanoparticles displayed the presence of aromatic signals at lower fields, with a chemical shift around 7.5 ppm associated with the protons of the aromatic groups of the covalently attached mesogen (Figure S1), whereas these signals were not present in the spectrum of SiO$_2$-NH$_2$.[9] From the TGA analysis (Figure S2), the SiO$_2$-OH nanoparticles had a total loss of 1.78 wt%, which is associated to the presence of silanol groups on their surface. The TGA curve of the SiO$_2$-NH$_2$ presents one decomposition step at ~410 °C related to the chemical attachment of APTES molecules onto the surface. The total weight loss was 6.65 wt%, indicating that ~4.8 wt% of APTES was attached to the SiO$_2$ nanoparticle surface. In contrast, the TGA plot of the M-SiO$_2$ nanoparticles displays a two-step degradation curve, indicating progressive decomposition of surface groups, one due to the mesogens at ~220 °C and the other due to the APTES groups at ~410 °C; and the total loss was 9.74%.

The M-SiO$_2$ nanoparticles exhibited fluorescence at certain UV range, which could be used as a simple technique to monitor the presence of the SiO$_2$ nanoparticles in solution, as demonstrated in Figure 1a. The SiO$_2$-OH nanoparticles were water soluble whereas the M-SiO$_2$ nanoparticles were soluble in organic solvents after surface modification. UV-induced fluorescence clearly demonstrates good dispersion of M-SiO$_2$ nanoparticles in the organic solvent. Transmission electron microscope (TEM) images (Figure 1b) also showed apparent well-dispersion of M-SiO$_2$ nanoparticles, demonstrating no noticeable aggregation in solution compared with the precursor SiO$_2$-OH and SiO$_2$-NH$_2$ nanoparticles. The serious overlap of SiO$_2$-OH nanoparticles was observed in the TEM grid due to the strong hydrogen bonding of the silanol groups. In contrast, when the mesogen was linked, no nanoparticle overlap was observed in the TEM image, which indicates the improvement of nanoparticle dispersion. The size of the M-SiO$_2$ nanoparticles was 26.97±2.92 nm, calculated by TEM considering 500 nanoparticles. The size distribution is showed in Figure S4 (top). Additionally, the presence of the nitrogen, oxygen and silicon in the functionalized

nanoparticles was observed from energy dispersive X-ray (EDX) spectrum (see the supporting information Figure S4 (bottom)).

To explore the effect of M-SiO$_2$ nanoparticles on the properties of DFCLC host, 0.5, 1.0, 1.5, 2.0 and 3.0 wt% M-SiO$_2$ nanoparticles were respectively doped into the DFCLC with a pitch length of around 1.6 μm. The DFCLC used here is comprised commercially available chiral dopant S811 (6 wt%) and 94 wt% nematic DFLC (DP002-016, T_{N-I} = 104 °C, n = 0.268). The M-SiO$_2$ doped DFCLC nanocomposites were capillary-filled into the LC cells assembled from untreated glass substrates with 15 μm cell gap. Their liquid crystalline behaviors at room temperature were observed under a polarized optical microscopy (POM) with crossed polarizers in transmission mode. At the initial state, all cells displayed typical oily streak cholesteric textures (Figure 2). No evident aggregates were observed in the POM textures of the nanocomposites, suggesting that the M-SiO$_2$ dispersed homogeneously in the DFCLC host even when the M-SiO$_2$ concentration was increased up to 3.0 wt% (Figure 2f). It was found that the cholesteric (N*)-isotropic (I) and I-N* phase transition decreased with the increase of nanoparticle concentration as shown in Supporting Information Figure S5. One possible explanation of these observations is related to the decreased ordering in the DFCLC matrix after doping the M-SiO$_2$ nanoparticles in the medium, as reported before for other nanocolloidal systems.[10]

The electro-optical properties of M-SiO$_2$/DFCLC nanocomposites were further investigated by applying an AC field at different frequencies and a constant voltage of 20 V. Figure 3 displays the POM textures of 2 wt% M-SiO$_2$ doped DFCLC and pure DFCLC host with different frequencies at a constant voltage. As it can be observed, at the low frequency of 0.1 kHz, a homeotropic texture (Figure 3a and 3d) was formed, where the helix was unwound by a dielectric coupling between LC molecules and the vertical electric field. The inset shows the conoscopic interference pattern with a Maltese cross, confirming the existence of the molecular alignment perpendicular to the substrate, *i.e.*, homeotropic (H) state. Upon increasing the frequency to 30 kHz, a focal conic (FC) texture was developed (Figure 3b and 3e), and the light was scattered due to the random orientation of the helical axes of the DFCLC domains. When the frequency was further increased to 70 kHz, the LC arrangement transformed into a planar state where the helical axis is perpendicular to the substrates of LC cell (Figure 3c and 3f). The transmittance and contrast ratio of DFCLC nanocomposites with different concentrations of M-SiO$_2$ nanoparticles were evaluated through the transmission spectra detected by a fiber-optic spectrometer. The higher and lower transmission intensities were defined as I^+ in the homeotropic state and I^- when the light source was extinguished; the contrast ratio (CR) was defined as CR=T^+/T^- where T^+ was assigned to the transmission intensity in the homeotropic state and T^- was assigned to transmission of the FC or the planar state. As shown in Figure 4a, an improved contrast ratio for all M-SiO$_2$ doped DFCLC nanocomposites compared with the pure DFCLC host was attained. Nevertheless, in the planar state (higher frequencies), the transmittance decreased with the increase of the M-SiO$_2$ content (Figure 4b), which enabled a partially transparent state.

Figure 5 shows the photographs of a colorful image behind the two LC cells respectively containing 2 wt % M-SiO$_2$ doped DFCLC (top) and the pure DFCLC host (bottom) in the H (transparent), FC (scattered) and planar states (partially transparent). The colorful image

(yellow sphere, red helix and space-filling model of surfactants on black-doted blue background) behind both LC cells can be clearly observed at low frequency (Figure 5a and 5d, 0.1 kHz, H state), whereas when a higher frequency was applied (Figure 5b and 5e, 30 kHz, FC) the colorful image behind both cells was not visible due to light scattering of the FC domains. However, for the DFCLC thin film containing 2 wt% M-SiO$_2$, the scattering is greatly enhanced and the colorful image behind the cell cannot be perceived due to the stronger scattering effect from the embedded nanoparticle system. When a higher frequency was applied, both the pure DFCLC and M-SiO$_2$ doped DFCLC reconfigured into the planar state (Figure 5c and 5f, 70 kHz, planar state), however the M-SiO$_2$ doped sample was partially transparent due to the influence of silica nanoparticles in the helical arrangement in the LC cell. It is noteworthy that both P and FC states were found to be stable for a long period of time even when the applied field was removed, since no noticeable change in the states, *i.e.*, partially transparent and opaque, was observed (Figures S8 and S9).

To have a clear insight about the possible arrangement of LC molecules in the M-SiO$_2$ doped DFCLC and the pure DFCLC, a schematic representation of the M-SiO$_2$ doped DFCLC nanocomposite and pure DFCLC is illustrated in Figure 6. At lower frequencies, the helix is unwound and the molecules tend to align parallel to the vertical electric field due to the LC exhibiting a positive dielectric anisotropy ($\varepsilon > 0$) where the homeotropic state is preferred (Figure 6 top). An increase in the frequency induced the cholesteric organization but the helical axes are randomly oriented resulting in the FC state, *i.e.*, scattered state (Figure 6 middle). When the frequency is further raised, the helical axes orient parallel to the electric field due to the LC exhibiting a negative dielectric anisotropy ($\varepsilon < 0$), assembling into the planar configuration (Figure 6 bottom). Doping M-SiO$_2$ nanoparticles might result in the increase of defect density in the helix configuration and subsequently a stronger light scattering due to the refractive index mismatching among FC multi-domains; other possible explanation of the achievement of higher contrast ratio could be attributed to the dynamic turbulence of the nanoparticles in LC media when subjected to the fields at higher frequencies, where an enhance of scattering is produced by localized variations in the index of refraction at both FC and planar states.

In summary, we have designed and functionalized silica nanoparticles with a covalently-attached mesogenic monolayer through a silane coupling agent. The resulting M-SiO$_2$ nanoparticles were soluble in organic solvents and characterized by ^{1}H NMR, TGA, UV-Vis, TEM, and EDX techniques. The organo-soluble M-SiO$_2$ nanoparticles were doped in a dual frequency cholesteric LC medium with different concentrations (0.5 wt%~3.0 wt%) exhibiting superior dispersion. From the electro-optical measurements, it was found that doping silica nanoparticles was able to greatly improve the contrast ratio of the nanocomposites compared with the pure DFCLC, which might result from the refractive index mismatching among FC multi-domains, and the dynamic turbulence of the nanoparticles in LC cell when subjected to the fields at higher frequencies. The optimal contrast ratio for both FC and planar states was achieved in 2 wt% M-SiO$_2$ doped DFCLC nanocomposite. Importantly, three stable states, *i.e.*, transparent, opaque, and partially transparent were accomplished by doping M-SiO$_2$ nanoparticles into the DFCLC under different frequencies at low applied voltage, which indicates that is possible to make devices with tunable transparency with such functional materials. This work disclosed here to

enhance scattering and reversibly control molecular orientation driven by frequency through hybrid nanoparticles offers an impetus in developing dynamic functional architectures and devices such as smart windows. Moreover, the synthetic route demonstrated here could provide an easy access to synthesize diverse surface-functionalized SiO_2 nanoparticles with desired properties, which could improve the properties of other liquid crystalline systems through nanoparticle-LC synergetic interaction.

Supplementary Material

Refer to Web version on PubMed Central for supplementary material.

Acknowledgments

References

1. a) Kitzerow, HS., Bahr, C., editors. Chirality in Liquid Crystals. Springer; New York, USA: 2001. b Zheng Z, Li Y, Bisoyi HK, Wang L, Bunning TJ, Li Q. Nature. 2016; 531:352–356. [PubMed: 26950601] Wang L, Li Q. Adv Funct Mater. 2016; 26:10–28.Bisoyi HK, Li Q. Angew Chem Int Ed. 2016; 55:2994–3010.

2. a) Xu M, Yang DK. Appl Phys Lett. 1997; 70:720–722.Hsiao YC, Tang CY, Lee W. Opt Express. 2011; 19:9744–9749. [PubMed: 21643231] Kumar P, Kang SW, Lee SH. Opt Mater Express. 2012; 2:1121–1134.Ma J, Shi L, Yang DK. Appl Phys Express. 2010; 3:021702.e) Cheng KT, Lee PY, Qasim MM, Liu CK, Cheng WF, Wilkinson TD. ACS Appl Mater Interfaces. 2016; 8:10483–10493. [PubMed: 27035635]

3. a) Bisoyi HK, Kumar S. Chem Soc Rev. 2011; 40:306–319. [PubMed: 21125105] Wang L, Gutierrez-Cuevas KG, Bisoyi HK, Xiang J, Gautam G, Zola RS, Kumar S, Lavrentovich OD, Urbas A, Li Q. Chem Commun. 2015; 51:15039–15042.Wang L, Gutierrez-Cuevas KG, Urbas A, Li Q. Adv Opt Mater. 2016; 4:247–251.Kumar R, Raina KK. Liq Cryst. 2015; 42:119–126.

4. a) Kreuzer M, Tschudi T. Appl Phys Lett. 1993; 62:1712–1714.Jákli A, Almásy L, Borbély S, Rosta L. Eur Phys J B. 1999; 10:509–513.Diorio NJ Jr, Fisch MR, West JW. Liq Cryst. 2002; 29:589–596.

5. Payne JC, Thomas EL. Adv Funct Mater. 2007; 17:2717–2721.

6. a) Li W, Zhu M, Ding X, Li B, Huang W, Cao H, Yang Z, Yang H. J Appl Polym Sci. 2009; 111:1449–1453.Kumar P, Raina KK. Opt Mater. 2012; 34:1878–1884.Hsu CJ, Kuo CC, Hsieh CD, Huang CY. Opt Express. 2014; 22:18513–18518. [PubMed: 25089470]

7. a) Rachet V, Lahlil K, Bérard M, Gacoin T, Boilot JP. J Am Chem Soc. 2007; 129:9274–9275. [PubMed: 17625865] Glushchenko A, Kresse H, Reshetnyak V, Reznikov Y, Yaroshchuk O. Liq Cryst. 1997; 23:241–246.c) Busbee JD, Juhl AT, Natarajan LV, Tongdilia VP, Bunning TJ, Vaia RA, Braun PV. Adv Mater. 2009; 21:3659–3662.

8. a) Xue C, Xiang J, Nemati H, Bisoyi HK, Gutierrez-Cuevas KG, Wang L, Gao M, Zhou S, Yang DK, Lavrentovich OD, Urbas A, Li Q. ChemPhysChem. 2015; 16:1852–1856. [PubMed: 26097118] Lewandowski W, Wójcik M, Górecka E. ChemPhysChem. 2014; 15:1283–1295. [PubMed: 24789440]

9. a) Nakahara Y, Takeuchi T, Yokoyama S, Kimura K. Surf Interface Anal. 2011; 43:809–815.Heintz AS, Fink MJ, Mitchell BS. Appl Organometal Chem. 2010; 24:236–240.

10. a) Gorkunov MV, Osipov MA. Soft Matter. 2011; 7:4348–4356.Gutierrez-Cuevas KG, Wang L, Xue C, Singh G, Kumar S, Urbas A, Li Q. Chem Commun. 2015; 51:9845–9848.
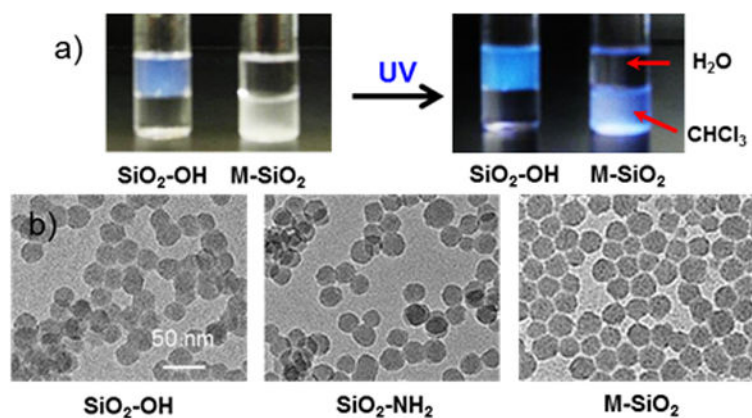
Figure 1.
(a) Photographs of SiO_2 nanoparticle solutions before (SiO_2-OH) and after ligand exchange (M-SiO_2) in a water-chloroform mixture with and without 365 nm UV irradiation, and (b) TEM images of SiO_2-OH, SiO_2-NH_2 and M-SiO_2 nanoparticles.
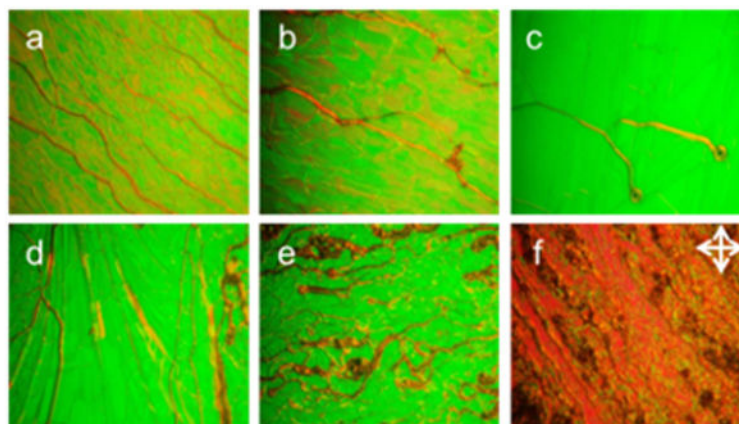
Figure 2.
POM textures of DFCLC nanocomposites with different concentration of M-SiO$_2$ nanoparticles at 0 wt% (a), 0.5 wt% (b), 1.0 wt% (c), 1.5 wt% (d), 2.0 wt% (e) and 3.0 wt% (f) at room temperature.
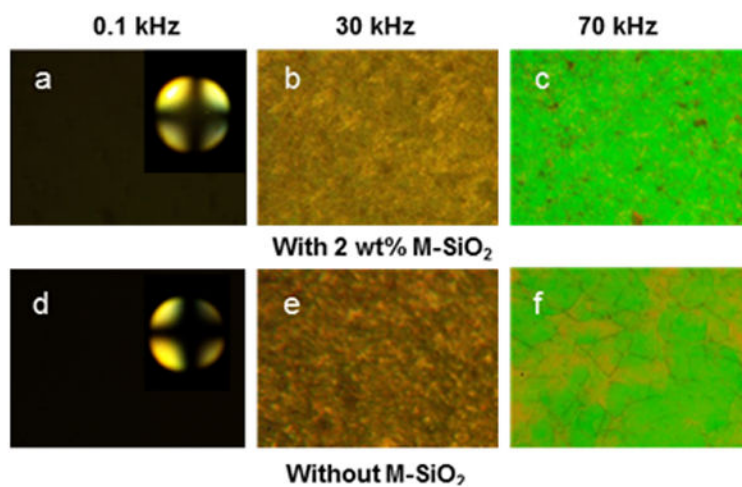
Figure 3.
POM textures of DFCLC with 2 wt% M-SiO$_2$ and without M-SiO$_2$ at 0.1 kHz, 30 kHz and 70 kHz under an applied constant voltage of 20 V.
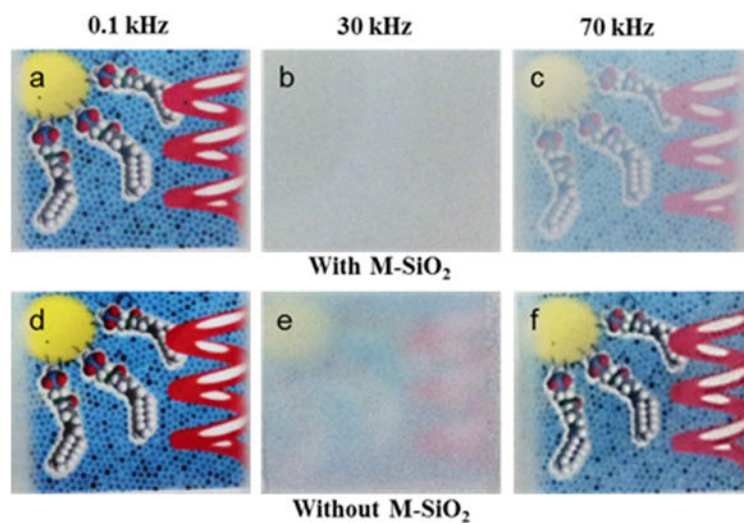
Figure 4.
Contrast ratio (black) and transmittance (blue) curves of incident light (550 nm) with different concentrations of $M-SiO_2$ nanoparticles in DFCLC at (a) focal conic state (30 kHz, 20V) and (b) planar state (70 kHz, 20V).

Figure 5.
Photographs of a colorful image positioned behind the LC cells containing DFCLC with 2 wt% M-SiO$_2$ (a, b, c) and without M-SiO$_2$ (d, e, f) at 0.1 kHz, 30 kHz and 70 kHz respectively under an applied constant bias of 20 V.
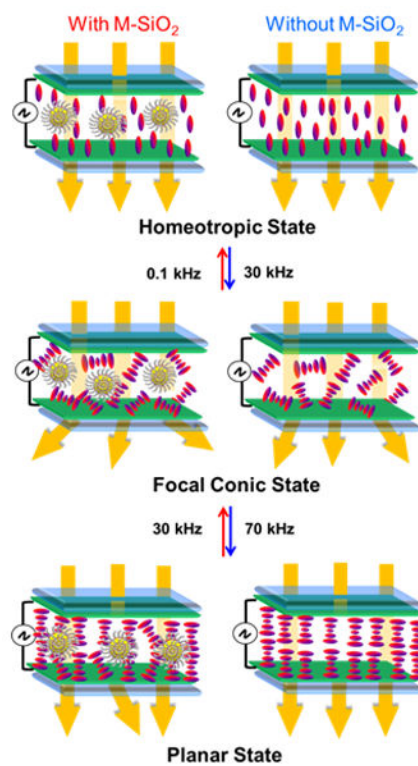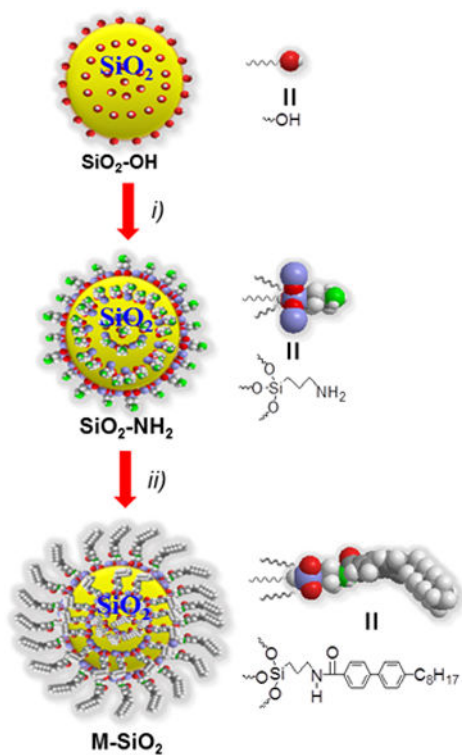
Figure 6.

(a) Schematic illustration of M-SiO$_2$ doped DFCLC nanocomposite (left) and pure DFCLC (right) in the LC cell at three different states driven by different frequencies but under constant voltage.

Scheme 1.
Synthesis of mesogen-grafted silica nanoparticles (M-SiO$_2$). i) (3-amino propyl)-triethoxy silane, ethanol, and ii) 4-octyl-4-biphenylcarboxylic acid, N-(3-dimethylaminopropyl)-N-ethylcarbodiimide hydrochloride, THF.